Gelation and Rheological Properties of Ultrasound-Extracted Faba Bean Protein: A Comparative Study with Commercial Plant Proteins

BADJONA, Abraham, CHERONO, Beatrice, BRADSHAW, Robert and DUBEY, Bipro <http://orcid.org/0000-0003-0396-9864>

Food Hydrocolloids 162 (2025) 110997

Contents lists available at ScienceDirect

Food Hydrocolloids

journal homepage: www.elsevier.com/locate/foodhyd

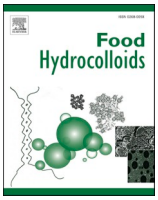

Gelation and rheological properties of ultrasound-extracted faba bean protein: A comparative study with commercial plant proteins

Abraham Badjona [a], Beatrice Cherono [a], Robert Bradshaw [b], Bipro Dubey [a,c,*]

[a] National Centre of Excellence for Food Engineering, Sheffield Hallam University, Sheffield, S1 1WB, UK
[b] Bimolecular Research Centre, Sheffield Hallam University, Sheffield, S1 1WB, UK
[c] School of Engineering and Built Environment, College of Business, Technology and Engineering, Sheffield Hallam University, Sheffield, S1 1WB, UK

ARTICLE INFO

Keywords:
Rheology
Gelation
Plant protein
Biopolymer
Plant-based foods
Ultrasound-extracted faba bean protein (US-FBP)

ABSTRACT

Environmental and consumer concerns about dependence on animal-based proteins have sparked interest in sustainable alternatives, with plant-based biopolymers emerging as a promising substitute. The present study comprehensively assessed and compared the rheological and structural properties of commercial plant proteins (pea and soy) and ultrasound-extracted faba bean protein (US-FBP) to provide an extensive overview of their comparative characteristics. At 12 % protein concentration, the exponent n approached zero for soy ($n = 0.32$) and pea ($n = 0.56$), whereas it remained higher for faba bean protein ($n = 0.69$) after fitting a viscosity curve to power law model. The least gelation concentration was observed to be 10 % for US-FBP, soy and pea protein. Additionally, in situ gelation indicated strong gel formation by soy (loss factor = 0.19) compared to US-FBP (0.24) and pea protein (0.37). Secondary structure analysis using FTIR spectroscopy and water/oil absorption capacity measurements revealed significant differences between these proteins. This opens interesting possibilities for using a wide range of plant proteins in the design, formulation, and customization of next-generation plant-based foods.

1. Introduction

The interest in the plant-based food industry is gaining increasing attention with plant-derived alternatives to standard meat and dairy products becoming established options. Research has demonstrated that plant-based diets, which include plant proteins, can provide significant nutritional benefits while also enhancing environmental sustainability (Magrini et al., 2018). The health benefits associated with consumption of plant-based diets are notable and are key areas of scientific interest. Lescinsky et al. (2022) revealed that diets characterized as vegetarian and prudent, which include small quantities of red meat, are correlated with a reduced risk of diseases, notably heart disease and type 2 diabetes. The production of food through livestock farming significantly contributes to emissions of greenhouse gases, depletion and degradation of resources, and biodiversity losses (Hayek, Harwatt, Ripple, & Mueller, 2021). Annually, billions of animals are bred and slaughtered for food, frequently experiencing unfavourable conditions (Weathers et al., 2020). Large-scale animal production in factory farms heightens the danger of zoonotic diseases and antibiotic resistance, posing a significant threat to both the global economy and public health (Stevenson, 2023). Despite the increase in plant-based alternatives in many countries, the consumption of animal-based proteins remains predominant.

Presently, the majority of proteins utilized as functional ingredients in plant-based foods are derived from a limited number of sources, including soybeans, peas, wheat, and corn. Nonetheless, many other protein sources can be utilized to formulate these products, potentially providing new or improved functional properties, such as thickening and gelling agents as well as for foaming or emulsifying (Paximada et al., 2021). For example, proteins displaying these functional characteristics can be extracted from faba beans (Badjona et al., 2024c), tubers, nuts, cereals (Kaur et al., 2022) and a variety of other sources. Globulins are the major storage proteins of pulses constituting between 35 and 80 % of the total protein content. The major structural composition and functionality of different pulse globulins has been extensively investigated in previous research (Sim et al., 2021) and have been shown to have numerous applications in the food industry. Moreover, it is now apparent that isolation methods and downstream processing can alter

* Corresponding author. National Centre of Excellence for Food Engineering, Sheffield Hallam University, Sheffield, S1 1WB, UK.
E-mail addresses: a.badjona@shu.ac.uk (A. Badjona), beatricecheronob@gmail.com (B. Cherono), r.bradshaw@shu.ac.uk (R. Bradshaw), b.dubey@shu.ac.uk (B. Dubey).

https://doi.org/10.1016/j.foodhyd.2024.110997
Received 26 October 2024; Received in revised form 3 December 2024; Accepted 16 December 2024
Available online 17 December 2024

the functionality of plant proteins, resulting in isolates with the same [percent/level] of protein but displaying very different properties (Schlangen et al., 2022a). The protein source is also a determinant factor defining the textural properties of milk and meat analogues that drives consumer preferences (McClements, 2023). For instance, soy protein and wheat gluten provide a more fibrous structure and elastic texture than pea protein (Snel et al., 2022). However, since wheat and soy are major food allergens (Coimbra, Costa, Evangelista, & Figueiredo, 2023), the use of pulse proteins, e.g., peas, mung beans, and fava beans, is recently gaining importance (Badjona et al., 2023; Mazumder et al., 2023).

The apparent viscosity of suspensions in high-moisture biopolymer systems has been used to elucidate structure-function relationships (McClements, 2023; McClements et al., 2019). The viscoelastic and gelling properties of globular proteins are influenced by numerous complex factors, making a thorough understanding of these interactions essential for food applications. Rheological properties, including shear viscosity for fluids and elastic modulus and fracture properties for solids, significantly affect the production quality, storability, and sensory aspects of next-generation plant-based foods (Kyriakopoulou et al., 2019). Conversely, using plant-based proteins from various sources as gelling agents can enhance overall sustainability, provide broader functionality in gelation, water-holding capacity, and emulsification, offer consumers a wider selection, and provide health benefits (Ma et al., 2022a). The necessity for a deeper understanding in this field is emphasized by the observation that many consumers attribute their low acceptance of plant-based analogues to undesirable textural and sensory qualities (Michel, Hartmann, & Siegrist, 2021).

The functional performance of various plant proteins can differ significantly between suppliers and batches (Jiménez-Munoz et al., 2023), complicating the formulation of commercial food products with consistent quality attributes. Therefore, this article focuses on understanding, predicting, and controlling the rheological characteristics of next-generation plant-based foods by: (i) investigating protein systems in the dilute biopolymer regime using viscosity measurements, (ii) analysing the viscoelastic behaviour of different protein dispersions, (iii) studying the minimum gelation concentration, (iv) examining the gelation mechanism through temperature sweeps, and (v) elucidating structural differences and water-holding capacity. This knowledge is expected to provide new opportunities for the diverse use of plant proteins in the development, design, and production of higher-quality plant-based products.

2. Materials and method

2.1. Raw materials and chemicals

Faba beans were sourced from Whole Foods Earth (Kent, United Kingdom). Sodium hydroxide (NaOH, ≥99.9 % purity) and hydrochloric acid (37 %) (HCl) were obtained from Sigma-Aldrich (UK). The seeds were finely milled using a Retsch twister cyclone mill at 12,000 rpm (sieve size of 0.5 mm) and stored at −20 °C until required. The particle size of the milled flour ca be found in our previous work (Badjona et al., 2024c). Three different commercial proteins were procured from various suppliers: pea and soy protein isolates from Pulsin Co. Limited (UK) and whey protein isolate from Myprotein (UK) as shown in Table 1.

2.2. Preparation of protein solutions

Pea, US-FBP, and soy proteins were dissolved in deionized water to obtain stock solutions at 12 and 10 % (w/v) concentration at 4 °C and stirred gently with a magnetic stirrer overnight. Within the first 2 h, the pH was adjusted to 7 using 1 M NaOH or HCl. The protein solutions were then diluted from the stock solution to concentrations of 10, 7, 5, and 4 %, with the pH readjusted to 7 after dilution (Table 2). The samples were prepared based on protein mass fraction.

Table 1
Chemical composition of plant protein used in this work.

Protein	Fat (%)	Carbohydrate (%)	Fibre (%)	Protein (%)	Salt (%)	Source
Soy	1.5	1.8	–	90	0.5	Plant (commercial)
Pea	9.1	0.2	1.4	80	4.90	Plant (commercial)
Whey	7.5	4.0	–	82	0.50	Animal (commercial)
US-FBP	nd	nd	nd	92	nd	Plant (Laboratory)

NB: Whey contained Soya lecithin and sunflower lecithin emulsifiers. nd: not determined.

Table 2
Nomenclature and formulation of protein suspensions from soy, pea and faba bean proteins.

Protein	Protein mass concentration (w/v %)	Total mass fraction (g)	Aqueous (mL)
Soy	12	13.33	86.67
	10	11.11	88.89
	7	7.78	92.22
	5	5.56	94.44
	4	4.44	95.56
Pea	12	15	85
	10	12.5	87.50
	7	8.75	91.25
	5	6.25	93.75
	4	5	95
US-FBP	12	13.04	89.96
	10	10.87	89.13
	7	7.61	92.39

2.3. Extraction of ultrasound-assisted faba bean protein isolate

Under the optimal conditions—power of 123 W, solute/solvent ratio of 0.06 (1:15 g/mL), sonication time of 41 min, and total volume of 623 mL—yielded a maximum extraction efficiency of 19.75 % and a protein content of 92.87 %, as established in a previous study (Badjona et al., 2024a, Badjona et al., 2023). For this study, faba bean flour was dispersed in water at a solute/solvent ratio of 0.06 (1:15 g/mL) with a total volume of 623 mL. The dispersion was agitated at 25 °C for 20 min at 500 rpm prior to ultrasonic-assisted extraction. The pH was adjusted to 11, followed by ultrasonic treatment at 123 W for 41 min using a S24d22D titanium ultrasonic horn (Teltow, Germany). The temperature was maintained between 20 and 25 °C using an ice bath. The mixture was then centrifuged at 25 °C for 20 min at 6000 rpm using an accuSpinTM 400 centrifuge (United Kingdom). The supernatant was collected, and the pH was adjusted to 4.0 with 1 N HCl while stirring continuously for 20 min. Protein isolate pellets were obtained by centrifugation at 6000 rpm for 20 min at 25 °C. The protein pellets were lyophilized for 48 h and stored at −20 °C for further analysis (Badjona et al., 2024b).

2.4. Viscosity

Protein samples were prepared as described previously and a concentration range between 12 and 4 % was used for measurement. Small deformation rheology was conducted using a rotational rheometer (MRC 302, Anton Paar, Graz, Austria) equipped with a 17 mm by 43 mm concentric cylinder with a gap of 1 mm (CC17/T200/SS) and an attached vane geometry (SR15-2V/2 V-32/100). The unit was temperature-controlled at 20 °C using an integrated water bath. Suspensions were added to fill the concentric cylinder to its maximum volume, and the viscosity of the samples was measured through a shear sweep ranging from 0.01 to 1500 s^{-1}. Each sample was analysed in replicates (n = 4), and the data was processed using RheoCompass

Software. Data was fitted to the power law model,

Apparent viscosity was calculated by the equation with the assumption that yield stress = 0,

$$\mu_{app} = K\dot{\gamma}^{(n-1)} \quad \text{eq. (1)}$$

were μ_{app} represents apparent viscosity (Pa·s), K is the consistency coefficient (Pa·s), $\dot{\gamma}$ is the shear rate (s^{-1}), and n is the flow behaviour index. Applying the log function to eq. **(1)**,

natural logarithm (ln) of both sides of equation (1):

$$\ln \mu_{app} = \ln K + \ln \dot{\gamma}^{n-1} \quad \text{eq. (2)}$$

$$\ln \mu_{app} = \ln K + (n-1)\ln\dot{\gamma} \quad \text{eq. (3)}$$

Eq. (3) *is* a linear equation considering $\ln\dot{\gamma}$ and $\ln \mu_{app}$ are independent (x) and dependent (y) variable, where $\ln K$ and (n-1) represents intercept and slope respectively. K (the consistency parameter) and n (flow behaviour index) can be estimated from experimental data.

2.5. Oscillatory measurement: amplitude sweep

Amplitude scanning was initially conducted to identify the linear viscoelastic region (LVR) of 12–20 wt% protein dispersions. A strain-sweep experiment was carried out at a constant frequency of 0.1 and 1 Hz at 20 °C. The storage modulus (G′) and loss modulus (G″) were measured across a strain range of 0.1–1000 % to determine the LVR for the different protein isolates.

2.6. Oscillatory measurement: frequency sweep

Small-amplitude oscillatory shear experiments were performed over an angular frequency (ω) range of 0.1–100 Hz at a constant strain rate of 0.2 % and a temperature of 20 °C, resulting in measurements of the storage modulus (G′) and loss modulus (G″). The strain amplitude of 0.2 % was chosen based on the amplitude sweep tests and was within the linear viscoelastic (LVE) regime for all samples under investigation. Protein dispersion used for this measurement was 12–20 wt%.

2.7. In situ gelation

Protein dispersions at concentrations of 12 and 15 wt% for rheometer testing were prepared as previously described. All samples were stirred overnight before rheological measurements. The rheological properties of the gels were tested using a rheometer equipped with a 17 mm by 43 mm concentric cylinder and attached vane geometry. The protein dispersions were carefully poured into the cup until the sampling area was filled, then covered with a thin layer of paraffin oil and a solvent trap to prevent water evaporation. Various tests were subsequently conducted on the samples.

(1) Temperature sweep (Gelation test): This involved heating the samples from 20 to 90 °C at a rate of 5 °C/min, holding them at 90 °C for 30 min, and then cooling them back to 20 °C at the same rate. The rheological parameters used to characterize the gels were the storage modulus (G′), loss modulus (G″), and the loss factor tan δ (G″/G′). G′ and G″ represent the elastic and viscous components of the viscoelastic behaviour, respectively, while tan δ describes the ratio of these two components. A material is considered a solid when tan δ < 1 and a strong solid when tan δ ≪ 1.
(2) Frequency sweep: the final gels were analysed using a frequency sweep spanning from 1 to 100 Hz, at a constant strain of 0.2 %.
(3) Strain sweep: a strain sweep was conducted while maintaining a constant temperature of 20 °C and a frequency of 1 Hz, with the strain ranging from 0.1 to 1000 %.

2.8. Least gelation concentration

The least gelation concentration was determined using a modified version of the method described by Kamani et al., (2024). Protein suspensions of varying concentrations (2, 4, 5, 7, 10, 12, 15 and 20 %) at pH 7 were prepared with a total volume of 20 mL each protein basis was used. The samples were then heated at 90 °C for 1 h, followed by cooling under running tap water. The cooled samples were subsequently incubated in the refrigerator (**4 °C**) for about 12 h. After gelation, a strain sweep was conducted while maintaining a constant temperature of 20 °C and a frequency of 1 Hz, with the strain ranging from 0.1 to 100 % to characterize the different gel strengths. Heat-set gels (12, 15 and 20 wt %) were placed on a rotational rheometer (MRC 302, Anton Paar, Graz, Austria) equipped with a parallel plate and a gap of 1 mm was used for strain sweep measurement.

2.9. Protein water holding capacity (WHC)

Water holding capacities were measured using a modified version of the method by Yang et al. (2023). Faba bean protein isolate (1.0 g) was dispersed in varying distilled water volumes (2, 5, 10, 12, 15 and 40 mL). The mixtures were vortexed for 1 min on maximum speed and allowed to stand for 2 h at room temperature (20–23 °C). Afterwards, the samples were centrifuged at 3000×g for 15 min at 20 °C and the WHC was estimated using eq. (4).

$$WHC = \frac{w_0 - w_1}{w_3} \times 100\ \% \quad \text{eq. (4)}$$

Where w_0 is the mass of the tube and protein isolate and absorbed water; w_1 is the mass of the tube and protein isolate while w_3 is the mass of faba bean protein.

2.10. Fourier-transform infrared spectroscopy analysis

An Attenuated Total Reflectance (ATR)-FTIR spectrophotometer (Spectrum 100 FT-IR, PerkinElmer, USA) was employed for the FTIR analysis. Spectroscopic measurements were performed with 16 scans at a resolution of 4 cm^{-1} over the range of 4000–650 cm^{-1}.

2.11. Statistical analysis

All statistical analyses were performed by Origin 2019 and excel 2024 (version 2406). All the values were expressed as means ± standard deviation (SD). All analysis was carried out in replicates except in situ gelation which was done in duplicate.

3. Results and discussion

3.1. Viscosity

The viscosity of biopolymer suspensions has been extensively studied to elucidate the structural and interactive dynamics within polymer mixtures (McClements, 2023). Additional studies are necessary to investigate the viscosity properties of different plant protein types. Viscosity, which is the measure of a fluid's resistance to flow, is directly affected by concentration, the strength of molecular bonds, and the morphology of the molecules in the suspension (Benoit, Afizah, Ruttarattanamongkol, & Rizvi, 2013). In certain instances, the viscosity of nonideal fluids varies with the duration of applied shear stress (Ansari, Rashid, Waghmare, & Nobes, 2020). The viscosity of protein suspensions was examined at various protein concentrations. The flow curves, representing viscosity as a function of shear rate for 12, 10, and 7 % solutions over a shear strain rate range of 1–1000 s^{-1}, are depicted in Fig. 1. Although the overall flow curves differed across protein concentrations, they all exhibited a shear-thinning behaviour. This trend

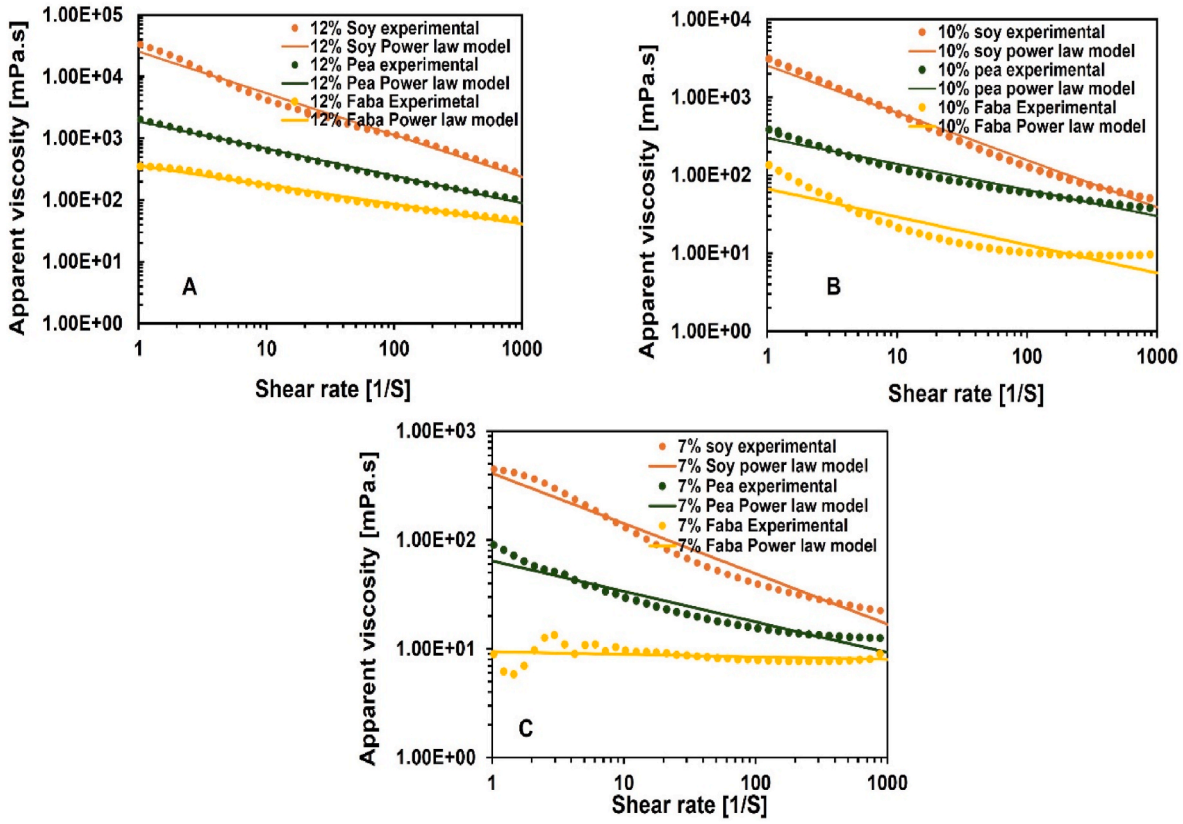

Fig. 1. Viscosity flow curves investigating different protein concentration (w/v) suspension of A) 12 % solution; B) 10 % solution; C) 7 % solution measured at 20 °C. Modelled with fits from the power-law is presented as solid lines, respectively. Each point is the average of 4 replicates.

aligns with other hydrocolloids reported in the literature and can be modelled using the power law equation. As illustrated in Fig. 1, the power law model fits reasonably for soy and pea proteins compared to faba bean proteins due to the complex structures of soluble and suspended proteins. At comparable protein concentrations, soy exhibited the highest viscosity, followed by pea protein, while faba bean protein suspensions demonstrated the lowest viscosity. In this present study, faba bean protein was found to have the lowest water-holding capacity compared to soy and pea proteins, which likely contributed to its reduced viscosity. Additionally, soy and pea proteins contain starch and fibre, which provide the structural integrity necessary to maintain viscosity even at low concentrations. The low viscosity of faba bean suspension could be advantageous for creating next-generation plant-based milk analogues with high protein content. Next generation plant based (NG-PB) milks typically consist of various particles or polymers suspended in an aqueous solution containing dissolved substances like sugars and salts. These products generally have a relatively low viscosity to mimic that of cow's milk (McClements, 2023; McClements & Grossmann, 2021).

Table 3 illustrates the power law fitting parameters of the protein solutions measured across the typical viscometer range of 1–1000 s^{-1}. It is evident that viscosity is influenced by polymer concentration. This analysis aimed to evaluate differences in flow behaviour and estimate the *K* and *n* values within this range, providing insights for rheometers with limited shear rate capabilities. All solutions exhibited shear-thinning behaviour, as indicated by the power law index (*n*) and consistency coefficient (*K*). The reduction in viscosity with increasing shear rate can be attributed to the entanglement theory. As shear stress causes disruption of the protein molecular structure, interactions between adjacent chains diminish. This behaviour is similar to that observed in certain milk or fluid egg analogues, where viscosity decreases with increasing shear rate due to the disruption of particles or polymers held together by weak forces (McClements et al., 2019). The model parameters for this range are summarized in Table 3. Additionally, the apparent viscosity at 100 s^{-1} representing the average shear rate in a n extruder for meat analogues is represented in Table 3.

Table 3
Power law model fitting parameters for the different protein solutions at 20 °C from shear rate of 1 - **1000** at 20 °C.

Protein isolate	Conc. (%)	K	n	(R^2)	μ_{ap} (mPa.s) at 100 s^{-1}
Soy protein	12	25424	0.32	0.98	1124.26 ± 110.98
	10	2542.5	0.39	0.99	59.26 ± 8.41
	7	410.52	0.55	0.99	15.44 ± 0.35
	5	68.001	0.69	0.98	6.36 ± 0.09
	4	32.993	0.74	0.9158	4.16 ± 0.06
Pea protein	12	1871.10	0.56	0.99	228.425 ± 4.35
	10	299.50	0.67	0.96	126.62 ± 11.31
	7	64.19	0.72	0.93	39.475 ± 1.43
	5	17.74	0.82	0.84	14 ± 0.50
	4	9.92	0.80	0.87	8.15 ± 4.03
Faba bean	12	362.74	0.69	0.99	79.20 ± 10.32
	10	66.99	0.64	0.85	10.10 ± 0.30
	7	9.40	0.98	0.11	7.89 ± 0.15

The coefficient of determination (R^2) was obtained from experimental data. Values of apparent viscosity are reported as mean ± standard deviation (n = 4). Values of viscosity at 100 s^{-1} were obtained from the experimental data.

These parameters exhibited trends consistent with those observed in the viscosity curves. All proteins demonstrated a concentration-dependent decrease in the power law index. Typically, greater shear thinning is observed at higher polymer concentrations due to increased polymer entanglement, which correlates with higher viscosity (Wittek et al., 2020). Shear thinning behaviour in globular plant proteins involves a marked reduction in the viscosity of a protein suspension as the

shear rate increases. This phenomenon occurs because applied shear stress disrupts protein-protein interactions and promotes the alignment of protein molecules within the suspension. The globular shape of these proteins facilitates their reorientation and mobility under shear, contributing to the observed decrease in viscosity (Liang, Wong, Pham, & Tan, 2016; McClements, 2023). Overall, increasing protein concentration led to an increase in K (consistency coefficient) and a corresponding decrease in n (power law index). The power-law parameters were derived by fitting the data from shear rates of 1–1000 s^{-1}, as depicted in the viscosity curves (log-log plot shown in Fig. 1). As protein concentration increased from 4 % to 12 %, the exponent n decreased from 0.74 to 0.32, approaching zero in the case of soy protein. A similar trend was observed for pea and faba bean proteins. At higher protein concentrations (12 % protein basis), the exponent n approached zero for soy ($n = 0.32$) and pea (n = 0.56), whereas it remained higher for faba bean protein ($n = 0.69$). As protein concentration decreases, so does the viscosity, as protein content is the primary determinant of the system's viscosity. Understanding the viscosity behaviour of protein suspensions is crucial for industrial applications, as it influences the design and optimization of various unit operations and processes in food product development.

3.2. Amplitude sweeps of protein dispersion

Viscoelastic materials can be categorized as either viscoelastic solids or liquids based on their response to applied stress. When stress is applied to a viscoelastic solid, it deforms at a finite rate until it reaches a fixed deformation, and upon removal of the stress, it gradually returns to its original dimensions. In contrast, a viscoelastic liquid continues to flow as long as the stress is applied and only partially recovers its original shape once the stress is removed. The rheological properties of viscoelastic materials are typically assessed by measuring their dynamic shear rheology (G) as a function of time, frequency, strain, or temperature. Amplitude sweep tests were conducted over a range of strains to evaluate both the linear viscoelastic (LVE) and non-linear viscoelastic (non-LVE) behaviour of these protein suspensions (McClements, 2023; Wittek et al., 2020).

The findings indicate that at low strain values, the biopolymer

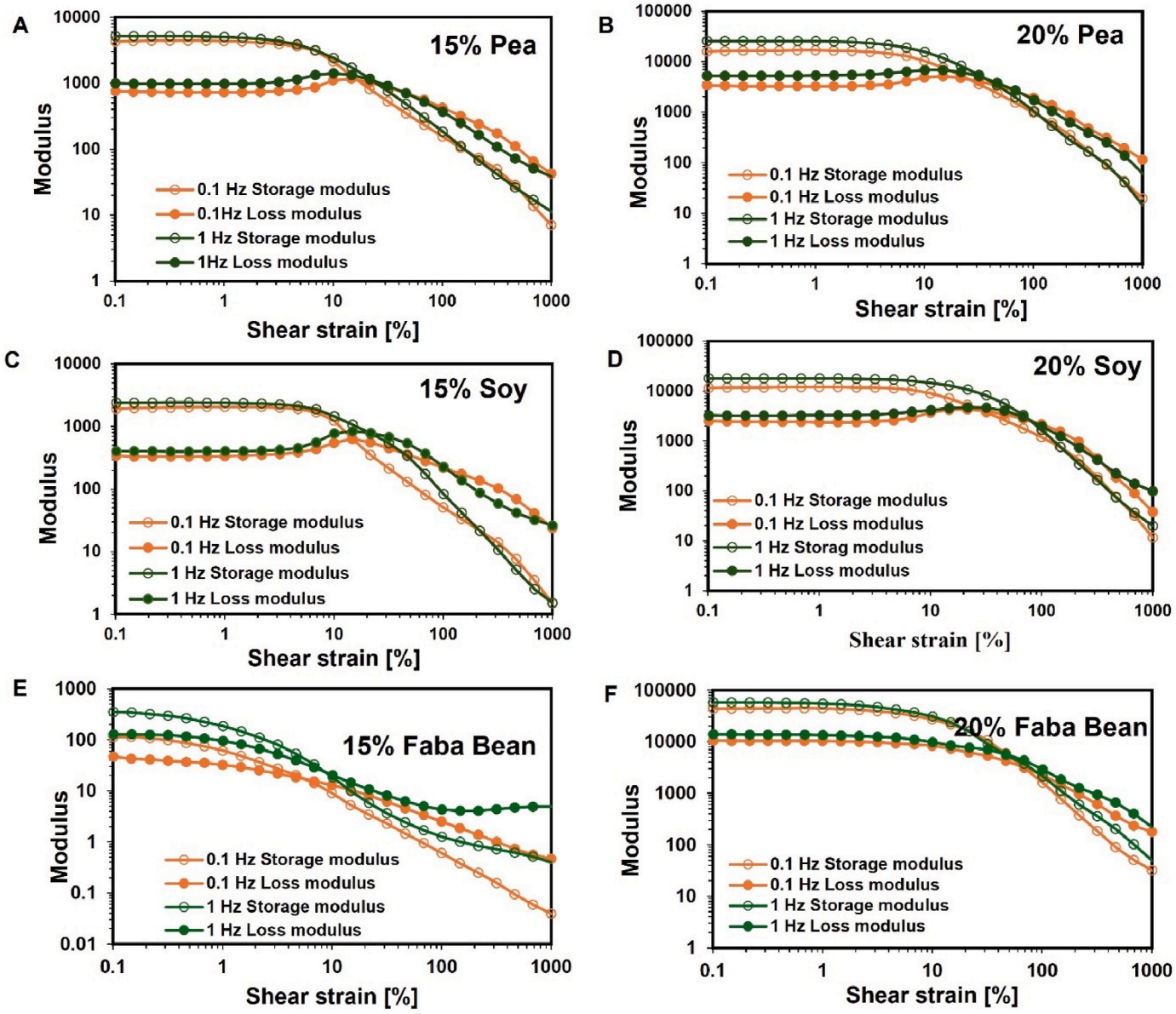

Fig. 2. Amplitude sweep test of **15 and 20 % wt**. protein suspension results demonstrate how the dynamic storage modulus (G′) and loss modulus (G″) vary with shear strain (γ) at constant frequencies of 0.1 Hz and 1 Hz at 20 °C.

suspensions demonstrate linear viscoelastic (LVE) behaviour, characterized by constant plateau values for both the storage modulus (G′) and the loss modulus (G″) within the low deformation range. As the strain exceeds the LVE regime, these protein suspensions exhibit a yield point and a cross-over point. The study observed at protein concentration of 15 and 20 % that both the storage and loss moduli remained relatively stable at low applied strains (<LVR) but decreased significantly when the strain exceeded approximately 1 % (Fig. 2). Typically, the storage modulus (G′) was higher than the loss modulus (G″) across the strain range of 0.1–10 %, except at a 12 % protein concentration for soy and US-FBP (data not shown). Generally, the modulus values were higher at 1 Hz compared to those at 0.1 Hz. At a 12 % protein concentration, soy protein exhibited the highest moduli, followed by US-FB protein, with pea protein showing the lowest. For the 15 % protein solution, pea protein displayed the highest moduli compared to soy and US-FBP protein. The critical yield strain at 12 % protein concentration was found to be less than 1%.

The yield strain values were approximately 1.48 % for pea protein, 3.18 % for soy protein, and 0.2 % for US-FBP at a concentration of 15%. A similar trend was observed at 20 % protein concentration, with yield strains increasing as the protein concentration rose. Specifically, at 20 %, the yield strain for pea protein was 2.17 %, for soy protein was 4.67 %, and for US-FBP was **1.01** %. The cross-over strain was found to be greater than 10 % for all samples at both 15 % and 20 % protein concentrations. The dynamic storage modulus (G′) and loss modulus (G″) of the protein dispersions increased significantly with higher protein concentrations. The constant plateau values at low strains suggest that these protein solutions behave predominantly as solid-like materials within this strain range. At higher deformation amplitudes, the G′ values decrease due to the disruption of the protein structure. The cross-over between G′ and G″ indicates a transition from solid-like to liquid-like behaviour.

3.3. Frequency sweep

Conducting both small-amplitude oscillatory shear (SAOS) and large-amplitude oscillatory shear (LAOS) experiments on protein suspensions with concentrations ranging from 12 to 20 % w/v allows for reliable identification and quantification of structural changes occurring during aggregation and breakdown, as well as approximation of processing-induced structural transformations. Rheological measurements of textural attributes in solid or semi-solid foods can provide valuable insights when changes in their properties are assessed in response to varying frequencies of applied oscillatory shear stress (Okeudo-Cogan et al., 2023). Frequency sweep tests, conducted over an angular frequency range of 0.1–100 Hz with a constant strain amplitude of 0.2 %, assess the stability of protein suspensions within this frequency range (Fig. 3). The amplitude sweep test confirmed that 0.2 % strain falls within the linear viscoelastic (LVE) region for all samples studied. Thus, frequency sweep tests offer insights into the stability of the protein suspensions at this constant strain amplitude across the measured frequency range.

The viscoelastic properties, represented by the dynamic storage modulus (G′) and loss modulus (G″), were plotted against oscillation frequency to assess how the yielding region evolves with increasing concentration (Fig. 3). At concentrations ranging from 12 to 20 %, the storage modulus consistently exceeded the loss modulus across the entire frequency spectrum, indicating that the protein suspensions predominantly exhibited elastic behaviour. A slight increase in both moduli was observed with increased frequency, likely due to the structural components of the proteins having less time to react to the oscillating stress at higher frequencies, resulting in greater resistance to deformation. At 12 % concentration, soy protein demonstrated the highest G′, followed by pea protein, with US-faba bean protein showing the lowest. On the contrary, at 20 % concentration, US-faba bean protein exhibited

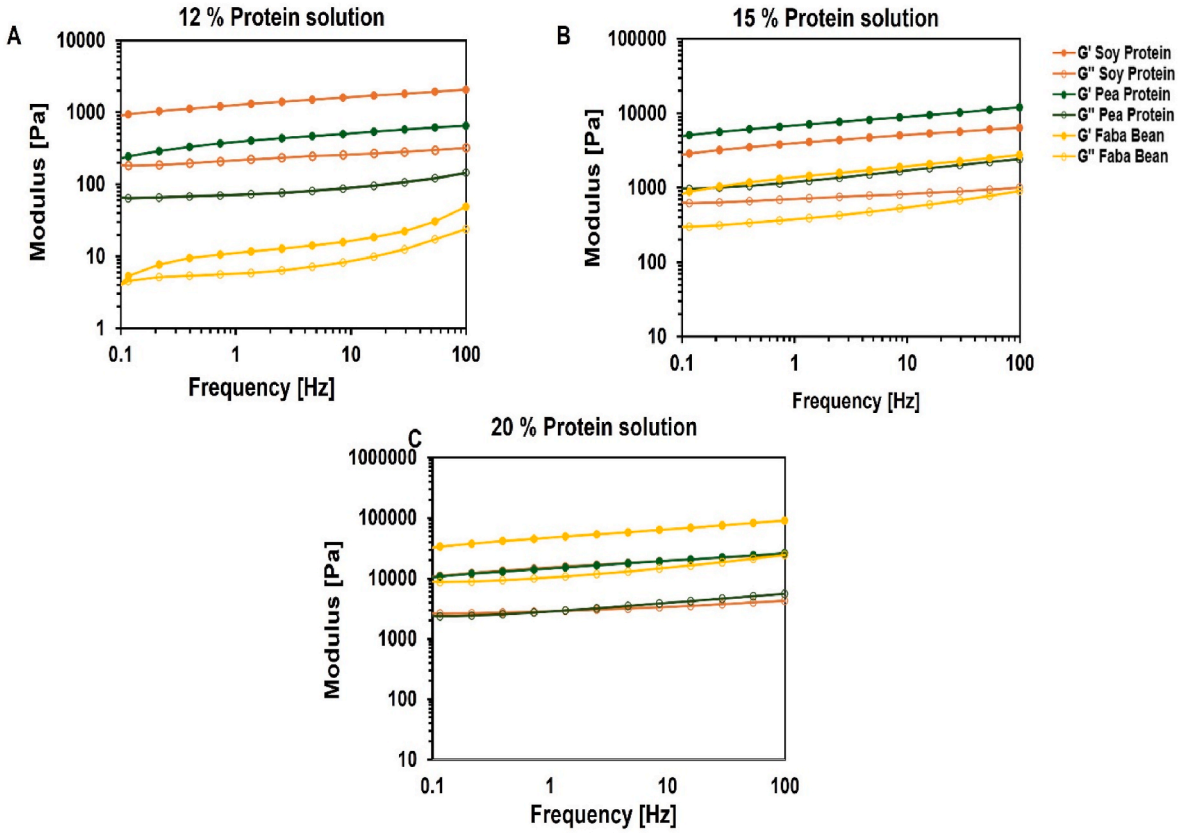

Fig. 3. The frequency sweep tests illustrate the changes in the dynamic storage modulus (G′) and loss modulus (G″) as a function of shear frequency for various protein suspensions, with a constant strain of 0.2 %.

the highest G′, followed by soy and pea proteins. We hypothesize that the observed improvement in G′ of US-FBP can be attributed to several factors. First, the high protein purity in US-FBP compared to soy and pea proteins likely reduced the influence of starch and fibres at lower protein concentrations (12 and 15 %), minimizing the "filler effect." Previous studies have indicated that even small amounts of starch can enhance the number of linkages within protein networks (Lyu et al., 2022). At a protein concentration of 20 %, the increased solid volume fraction may have contributed to the elevated G'. Additionally, the shear modulus of a suspension is influenced by the volume fraction of dispersed particles (φ), as described by the Eilers and Dijk equation, which links shear modulus to φ and introduces a maximum packing fraction (φ_m) for concentrated suspensions (Ferry, 1980). The φ_m value depends on particle size distribution and interparticle interactions. Therefore, we propose that enhanced protein-protein interactions, surpassing protein-water interactions, resulted in a denser, interconnected protein matrix at 20 % protein concentration, leading to higher shear modulus behaviour in US-FBP.

3.4. Least gelation capacity

The gelation behaviour of protein solutions was assessed by examining the least gelling concentration and rheological properties, as these factors are influenced by both molecular and colloidal interactions. The results for least gelling concentration were confirmed by both observation and strain sweep measurement are shown in Table 4. A gel was considered a weak gel if the gel was semi-solid while strong gels was considered self-supporting upon inversion. At a neutral pH of 7, a concentration of 10 % w/v was sufficient to form a self-standing gel for pea, soy, and ultrasound-extracted faba bean protein isolates. In contrast, a higher concentration of 12 % w/v was needed for whey protein to achieve gel formation. For soy protein isolate, concentrations of 15 and 20 % w/v produced strong gels; however, these gels exhibited breakage and slipping when inverted as shown in Fig. 4.

Strain sweep tests conducted over a broad strain range (0.1–100 s^{-1}) after heat-induced gelation revealed differences in the viscoelastic properties of the heat-set gels. Gels prepared with protein concentrations at 12–20 % exhibited a typical viscoelastic gel-like structure, characterized by G′ exceeding G″ throughout the strain range (Fig. 4) indicating the dominance of elastic properties. Notably, the rheological properties of the gels varied depending on the type of protein used. For 12% heat-set gels, whey protein displayed the highest G′, followed by soy and ultrasound-extracted faba bean proteins, with pea protein showing the lowest G′. As anticipated, increasing the protein concentration for all proteins to 15 and 20 % led to a noticeable increase in G′ for **all the studied proteins**. **All gels** at 12% protein concentration exhibited a yield strain of approximately 1.35 %, which increased to ~2.5 % at 15 % concentration (Fig. 4). The higher yield strains observed in soy and US-FBP gels compared to pea protein are consistent with findings reported in the literature (Hu et al., 2005; Shandet al., 2007).

The observed differences in gelation properties between soy protein isolate (SPI) and pea protein isolate (PPI) can be attributed to the distinct compositions of their globulin fractions. Soybean globulins, predominantly glycinin (11S) and β-conglycinin (7S), exhibit higher solubility compared to pea globulins, which are mainly legumin (11S) and vicilin (7S). At a higher protein concentration of 20 % w/v, US-FBP demonstrated a G′ comparable to that of whey protein, whereas soy and pea proteins exhibited lower G′ values. All heat-set gels at 20 % protein concentration displayed a similar yield strain of approximately 5%. For all protein types, the G′ was greater than G″, indicating successful gel formation. The gelation behaviour of plant proteins is influenced by multiple factors, including protein concentration, type, extraction and processing conditions, and the presence of other components such as starch, complex carbohydrates (fibres), and salts (Ma et al., 2022b; Tanger et al., 2021). Compositional differences among protein sources, such as varying levels of salts, fibers, and starch, can significantly impact and interfere with gelation. Proteins are primarily regarded as matrix formers when adequately hydrated, whereas other biopolymers, particularly complex polysaccharides found in unrefined ingredients like soy and pea, act as fillers, enhancing water retention within the matrix and influencing gel strength (van der Sman & van der Goot, 2023). Starch also plays a role in structure formation due to its water-binding capacity, which can modify gel strength depending on the starch type. During thermal processing, starch undergoes volume changes through swelling, gelling, degradation, and setting, further affecting gel characteristics (Bühler et al., 2022). High levels of fibres and starch in pea and soy proteins may partially entrap proteins within cellular matrices, reducing their availability for effective gel formation. In contrast, the high protein purity of US-FBP likely minimizes the presence of fibres and starch, reducing competition for water and facilitating the formation of stronger protein gel networks.

Table 4
Mapping of least gelation concentration of commercial plant-based protein isolates gels (heating at 90 °C for 1 h followed by cooling at 4 °C for 12 h).

Concentration (%)	Pea Isolate	Soy Isolate	U-Faba bean Isolate	Whey Protein
2	X	X	X	X
4	X	X	X	X
5	X	X	X	X
7	X	X	X	X
10	✓	✓	✓	▲
12	✓	✓	✓	✓
15	✓	✓	✓	✓
20	✓	✓	✓	✓

X no gel, ▲weak gel, ✓strong gel.

3.5. In situ gelation (temperature sweep)

Small amplitude oscillatory measurements examine the dynamic rheological properties without disturbing the internal network structure. Strain amplitudes in this range are too small to disrupt the gel microstructure, ensuring that the mechanical responses of gels in the linear viscoelastic (LVE) region remain unaffected by the applied stress or strain (Xia et al., 2022). For viscoelastic property measurements, an oscillatory strain of 0.2 % within the LVE range was used. During heat-induced gelation, the protein dispersions transitioned from a viscous liquid to a semi-solid, and eventually to a gel-like structure. The viscoelastic properties, specifically the storage modulus (G′) and loss modulus (G″), of the various protein dispersions (12 and 15%) were monitored as a function of temperature (heating from 20 to 90 °C and cooled to 20 °C). The heat-induced gelation process involved a cycle of heating, holding, and cooling (Fig. 5A). In viscoelastic materials, the storage modulus (G′) and loss modulus (G″) represent the elastic (non--dissipative) and viscous (dissipative) components, respectively (Mohamed et al., 2009). At all protein concentrations, US-FBP gels exhibited the highest G′ compared to pea and soy proteins. This indicates that US-FBP shows strong potential for use in meat analogue development through extrusion, even with high moisture content. This is due to its ability to form stronger gels at lower concentrations and temperatures (Xia, Siu, & Sagis, 2021). Among all the plant proteins studied, pea protein had the lowest G′ at both the beginning and end of the heating process, confirming the superior gelation behaviour of faba bean and soy protein isolates compared to pea protein isolates (Shrestha, Hag, Haritos, & Dhital, 2023). The differences in gel strength among the studied proteins can be attributed to several factors previously discussed. One key factor is the presence of constituents such as fibres and starch, which can modulate and interfere with the formation of robust protein gels. In pea and soy proteins, the high levels of starch and fibres, along with the diverse side groups present in these components, may lead to intramolecular interactions, cross-linking, and entanglement during gelation, potentially hindering the development of strong gels. Furthermore, the

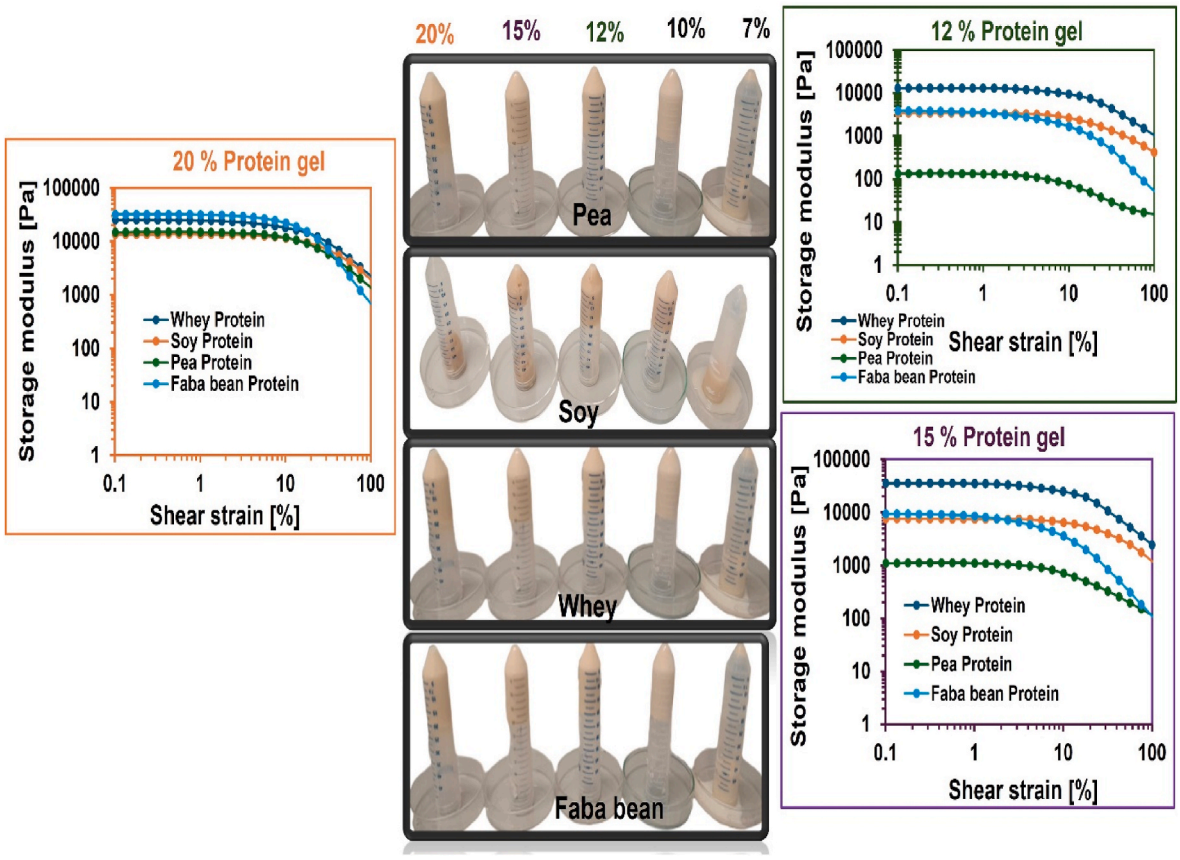

Fig. 4. Least gelation concentration with an associated strain sweep of heat set gels (heating at 90 °C for 1 h followed by cooling at 4 °C for 12 h). Strain sweep was performed after gel formation.

intrinsic properties of the protein types, such as differences in secondary structure and solubility, contribute to the distinct gelation behaviours observed for soy, pea, and faba bean proteins (Bora, Brekke, & Powers, 1994; Johansson, Karkehabadi, Johansson, & Langton, 2023).

Within the temperature range of 20–50 °C (Fig. 5B), the storage modulus (G') of US-FBP started lower than that of soy and pea proteins but gradually increased, surpassing pea protein as the temperature rose. This increase suggests that thermal softening in faba bean protein was likely offset by an increase in bond density, with a notable rise in G' occurring between 50 and 65 °C and an inflection point around 45 °C, indicating enhanced physical crosslinking dynamics that strengthen the network. For pea protein gels, network formation mainly relies on physical bonds such as hydrogen bonding and hydrophobic interactions between protein molecules (Sun & Arntfield, 2012), which intensify when proteins unfold due to heating. Pea protein formed spherical and hollow aggregates and particles, and heating above approximately 50 °C caused a steep increase in shear modulus due to protein unfolding and aggregation around the thermal denaturation temperature, forming a 3D elastic network. A similar observation was made for US-FBP and soy protein, where gel network formation in faba bean protein has been attributed to the exposure of initially buried hydrophobic groups during heating (Hall & Moraru, 2021). The gelation process is thought to proceed through several mechanisms: (1) protein denaturation, (2) formation of crosslinks between denatured proteins, (3) aggregate formation from these crosslinked proteins, and (4) continued aggregate growth leading to gel formation (Clark, Kavanagh, & Ross-Murphy, 2001). In less refined proteins such as soy and pea, the presence of components like fibres and starch can alter this gelation process, resulting in diverse gel structures. This is because the polarity and charge of biopolymers affect their interactions, including hydrophobic, hydrogen bonding, and electrostatic interactions, which are determined by the number of non-polar, polar, and charged groups in the biopolymer chains (McClements, 2023). These interactions significantly influence the structuring and gelling behaviour of the proteins.

Further heating caused a slight increase in shear modulus as more protein molecules unfolded and joined the network. Upon cooling from 90 to 20 °C, there was a significant increase in shear modulus, attributed to the strengthening of hydrogen bonds between protein molecules in the gel network.

The effect of heating and cooling on 15 % protein dispersions of the three plant proteins is shown in Fig. 6. A. The storage profile of 15 % dispersions of pea and soy proteins differed from the 12% storage profile. As observed in previous studies, the initial heating of 15 % pea and soy protein gels during the first 30 min (Fig. 6B) temporarily weakened the gels, but subsequent cooling restored their original strength, indicating the reformation of attractive forces between protein aggregates. Additionally, for proteins rich in thiol groups, the moduli can increase over time as the gel structure cools completely, due to the formation of disulfide bridges (Alting et al., 2003). However, for 15 % US-FBP, a similar trend to the 12 % gels was observed, with improved moduli. At the end of the cooling cycle for all 12 % protein gels, the values of G′, G″, and the loss factor were recorded to assess the gel strength of the proteins as shown in Table 5. Whey proteins exhibited the highest G′ at 2.48E+04 and the lowest loss factor of 0.17, indicating the formation of a very strong gel compared to plant-based proteins. Among the plant proteins, ultrasound-extracted faba bean (US-FBP) had the highest G′ of 2218 Pa with a loss factor of 0.24, while soy protein had a G′ of 1458 Pa and a loss factor of 0.19. Based on the loss factor, soy protein formed a relatively stronger gel than U-faba bean. Pea protein exhibited the lowest G′ at 236.27 Pa and a high loss factor of 0.373, indicating a weaker gel compared to soy and U-faba bean. For the 15 % gels, an increase in both G′ and G″ was observed at the end of the cooling cycle

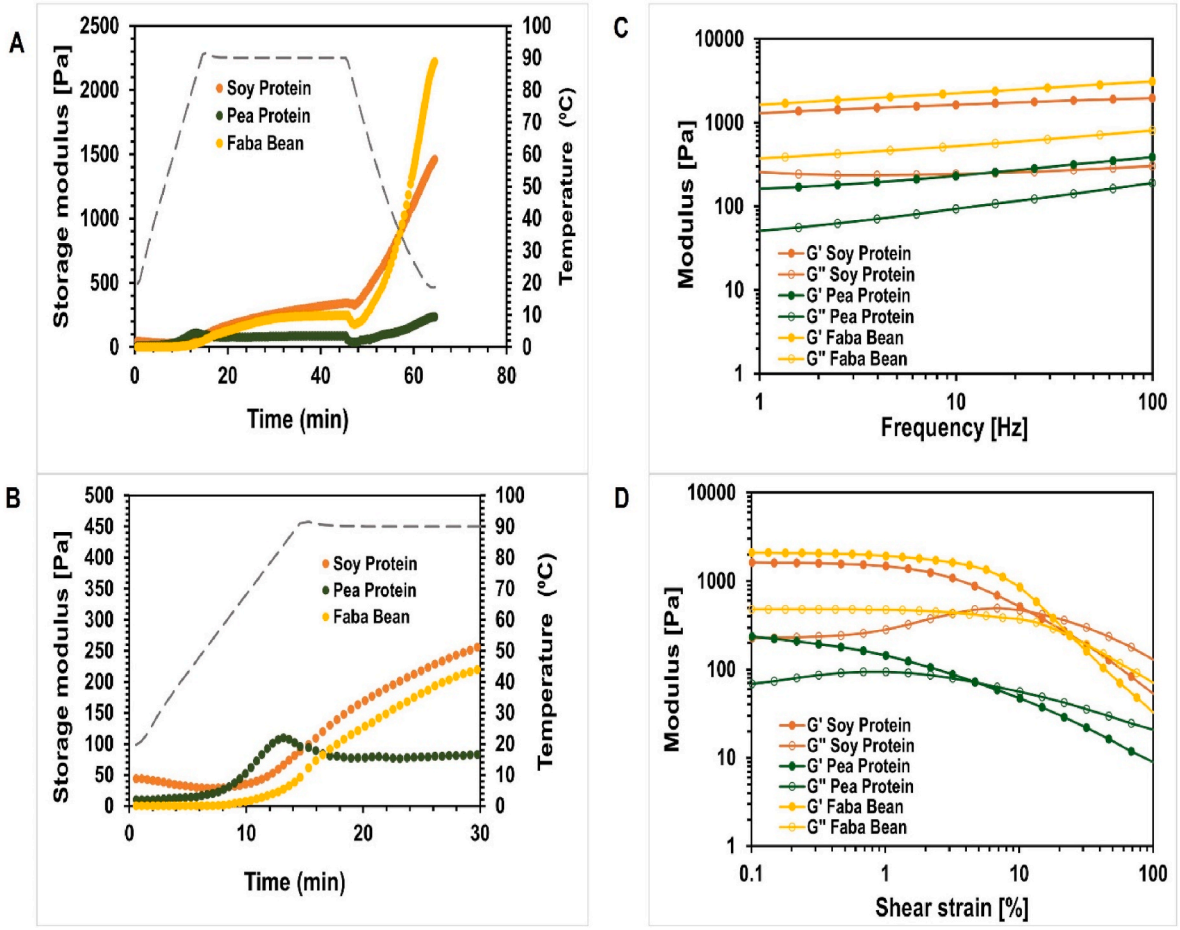

Fig. 5. (A) Temperature sweep (20–90 – 20 °C, f = 1 Hz, γ = 0.2 %) of gels formed at 12 % protein dispersion with temperature represented by dash line; (B) heating part of the temperature sweep (20–90 °C); (C) frequency sweep; and (D) strain sweep at 20 °C. G′ is indicated by filled symbols, and G" empty symbols.

for all proteins. US-FBP showed the highest G' (**6037.55** Pa) compared to soy (3107.8 Pa) and pea (2306.7 Pa) (Table 5). All the 15 % heat-set gels demonstrated a strong gel characteristic based on their loss factors (ranging from 0.18 to 0.22).

After completing the heating and cooling cycle, a frequency sweep (at a constant strain of 0.2 %) and an amplitude sweep (at a constant frequency of 1 Hz) were performed to further characterize the rheological properties of the gels, including their non-linear viscoelastic properties up to gel rupture. The gels exhibited distinct behaviours in the amplitude sweep (Fig. 5D & 6. D): they displayed a clear linear viscoelastic (LVE) regime at low strain. Beyond this regime, both G′ and G″ decreased due to the large shear strain causing partial rupture of the network bonds that stabilize the gel structure. From the amplitude test, two parameters were derived: the critical strain (γc) and the crossover strain (γG' = G″), along with the loss factor. The critical strain was defined as the shear strain at the end of the LVE regime, where the measured G′ value deviated by 5 % from the initial G′ value (Schlangen et al., 2022b). Beyond this point, the initial gel structure begins to break down. The crossover strain was defined as the point where the measured G′ value was last higher than the G″ value. These parameters together indicate the gel's ability to withstand deformation.

Focusing on the γ_c values (Table 6), whey protein gel showed the highest value of 3.18 %, indicating it can withstand significant deformation before rupturing. For 12% protein gels, the lowest critical strain was observed for pea protein (γ_c = 0.10 %), followed by soy (0.47 %), with US-FBP exhibiting the highest γ_c (1.34 %). A lower γ_c value indicated that pea and soy gels were easier to disrupt compared to US-FBP. Similar trends were observed for 15 % heat-set gels, with faba bean dispersion showing an improved critical strain (3.18 %) (**Table 6**). In combination with the γc results, materials with lower γc and γG' = G″ values had a more brittle texture and yielded sooner. When focusing on γG' = G″, US-FBP displayed a higher value (23.8 %) compared to soy (14.8%) and pea (4.67 %). Again, for 15 % dispersion, US-faba bean protein showed the highest γG' = G″ in comparison to pea and soy proteins. In combination with the γc results, one can interpret those materials with lower γc and γG' = G″ values had more brittle texture that yielded sooner. When focusing on γG' = G″, US-FBPf showed a higher value (23.8 %) compared to soy (14.8) and pea (4.67 %).

In the frequency sweeps (Fig. 5B & 6.B), the gels exhibited similar weak frequency dependence, indicating gel networks with very broad spectra of relaxation times (Ren, Xia, Gunes, & Ahrné, 2024). Additionally, the storage modulus (G′) of all protein gels was significantly higher than the loss modulus (G″) within the tested frequency range, confirming that the heat-set gels were predominantly elastic. This trend was also observed for the 15 % gelled proteins, which showed increased moduli. Both G′ and G″ of all the gels slightly increased with increasing frequency, with pea protein exhibiting the highest increase compared to soy and U-faba bean.

3.6. *Water holding capacity*

Water holding capacity (*WHC*) can serve as an indicator of protein state and functionality. The interaction of proteins with water is influenced by their amino acid composition and structure; proteins that hold more water tend to have higher levels of exposed hydrophilic groups and more charged amino acids (Ma, Grossmann, Nolden, McClements, &

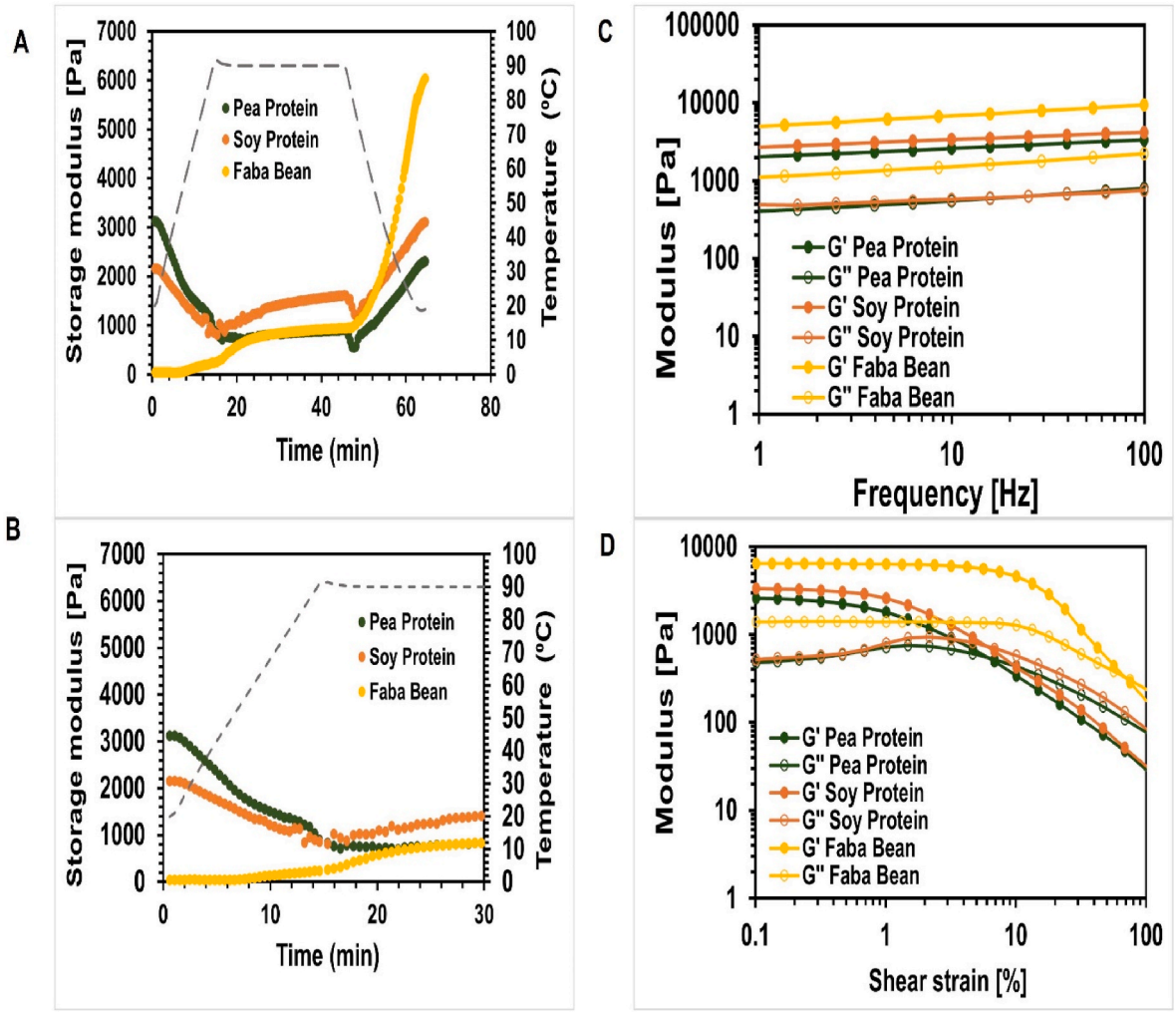

Fig. 6. (A) Temperature sweep (20–90 – 20 °C, f = 1 Hz, γ = 0.2%) of gels formed at 15 % protein dispersion, Temperature: dash line; (B) heating part of the temperature sweep (20–90 °C); (C) frequency sweep and (D) strain sweep at 20 °C. G': filled symbols; G": empty symbols.

Table 5
Measured G′, G″ and tanδ of heat induced gels at the end of the cooling cycle for different proteins suspensions (12 and 15 %).

Samples	G' (Pa)	G'' (Pa)	loss factor (tanδ)	Aspect
Soy Protein (12%)	1458.45 ± 60.74	274.60 ± 10.09	0.19 ± 0.02	Strong Gel
Soy Protein (15%)	3107.8 ± 431.06	541.94 ± 58.24	0.18 ± 0.01	Strong Gel
Pea Protein (12%)	236.27 ± 29.51	87.57 ± 0.32	0.37 ± 0.05	Weak Gel
Pea Protein (15%)	2306.7 ± 625.51	504.05 ± 107.33	0.22 ± 0.01	Strong Gel
Faba bean protein (12%)	2218.05 ± 431.69	540.07 ± 108.33	0.24 ± 0.00	Strong Gel
Faba bean protein (15%)	6037.55 ± 2375.81	1373.28 ± 547.62	0.23 ± 0.00	Strong Gel
Whey Protein (12%)	2.48E+04 ± 1448.16	4086.15 ± 272.17	0.17 ± 0.00	Very strong Gel

Table 6
Comparison of G', tan δ, γ_c and $\gamma G' = G''$ after performing strain sweep of 12 and 15 % heat induced gels.

Samples	G' (Pa)	tan δ	γ_c (%)	$\gamma G' = G''$ (%)
Soy Protein (12%)	1537.65 ± 48.44	0.17 ± 0.00	0.47	14.8
Soy Protein (15%)	3405.9 ± 346	0.15 ± 0.01	0.47	15.30
Pea Protein (12%)	236.025 ± 30.24	0.28 ± 0.02	0.10	4.67
Pea Protein (15%)	2660.7 ± 679	0.17 ± 0.00	0.10	6.85
Faba Bean (12%)	1880.55 ± 270.61	0.25 ± 0.0	1.34	23.8
Faba Bean (15%)	6053.75 ± 2183	0.23 ± 0.00	3.18	75.4
Whey Protein (12%)	21476 ± 1513.21	0.17 ± 0.00	3.18	217

Kinchla, 2022). As shown in Fig. 7, the *WHC* values for the three proteins varied significantly from protein/water ratio of 1:2 to 1:40. For all samples, *WHC* values increased with higher water addition, except at higher concentrations. The mean *WHC* for soy protein ranged from 1.52 to 7.38 g/g (Fig. 7C). A reduction in *WHC* was observed beyond a solute/solvent ratio of 1:25 g/mL, with no significant difference ($p < 0.05$) between ratios of 1:25 to 1:40 g/mL. Pea protein showed similar trends with some variations. The *WHC* of pea protein ranged from 1.64 to 4.75 g/g (Fig. 7B.), which was lower than that of soy protein. *WHC* increased from 1:2 to 1:20 g/mL, followed by a decrease from 1:25 to 1:35 g/mL. Significant differences ($p < 0.05$) in WHC were observed for pea protein at different solute/solvent ratios.

The *WHC* of US-FBP ranged from 1.80 to 4.06 g/g, with the highest

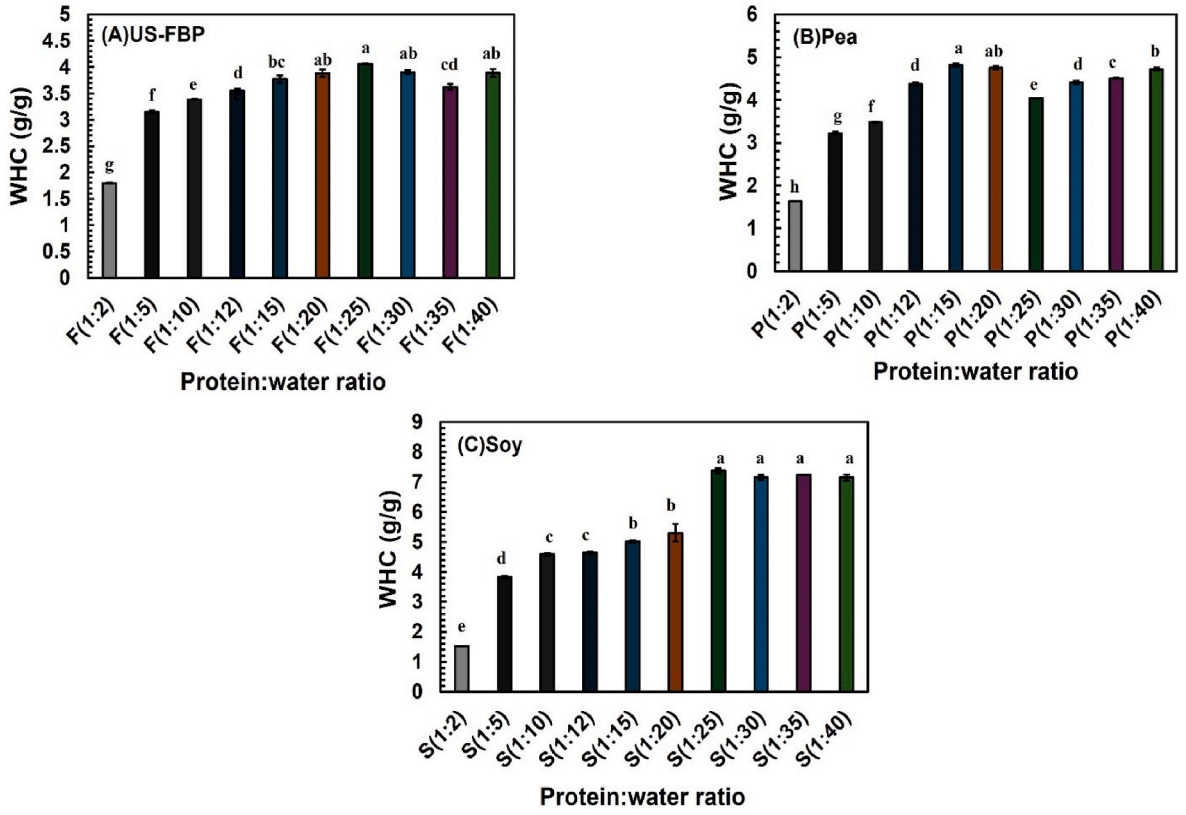

Fig. 7. Water holding capacity of (A) Faba bean protein isolate; (B) Pea protein and (C) Soy protein at different protein to water ratios. Values are reported as mean ± standard deviation (n = 3). The different letters denote significant differences ($P < 0.05$) between samples.

value (4.06 g/g) observed at a solute/solvent ratio of 1:25 g/mL. Significant differences ($p < 0.05$) were noted for the *WHC* of US-FBP across the different ratios ((Fig. 7. A.).). At the 1:25 g/mL ratio, soy protein exhibited the highest *WHC* (7.38 g/g), followed by US-FBP (4.06 g/g) and pea protein (4.05 g/g). The variations in WHC can be attributed to differences in extraction methods, ionic strength, amino acid composition, hydrophobicity, and protein conformation (Ma et al., 2022a; Ma et al., 2022).The slightly higher *WHC* of commercial soy protein compared to laboratory-extracted faba bean protein likely relates to their structural unfolding (Osen et al., 2014), which exposes more hydrophobic amino acids. Complex polysaccharides (fibres) in less refined plant-based ingredients like soy and pea proteins are primarily described as fillers that contribute significantly to water-holding capacity (*WHC*) (van der Sman & van der Goot, 2023). Starch is also recognized for its strong water-binding properties. The high WHC of soy proteins has been attributed to protein subunits such as glycinin and β-conglycinin, which exhibit high water-binding capacity due to their elevated levels of polar amino acids (Schmid et al., 2024). Additionally, other components in soy protein, including starch, may further enhance its overall *WHC*. In contrast, the slightly lower WHC observed in pea protein compared to soy and US-FBP may result from higher levels of fiber and fat, which could negatively influence *WHC* (Farshi et al., 2024). It has been shown that depending on the type of fibre, starch and fat, *WHC* can be either negatively or positively impacted (Nagy, Máthé, Csapó, & Sipos, 2021).

3.7. Fourier transform infrared spectroscopy (FTIR)

ATR-FTIR is a technique frequently utilized to examine conformational differences among proteins (Tiernan et al., 2020). Analysis of the spectra reveals significant variations in absorption across the entire range of wavenumbers. Average spectra were obtained, displaying the characteristic band distribution of different plant protein isolates (Fig. 8). Pea and soy proteins exhibited the most similar overall spectra, while U-faba bean and whey proteins had distinct spectra. All protein samples showed major peaks in the Amide I, II, III, A, and B regions. Notable differences in intensity among the proteins were observed in the amide regions and the fingerprint region (1800 - 1200 cm^{-1}) between US-FBP compared to commercial proteins (soy and pea) (Fig. 8B). The Amide I region (1600–1700 cm^{-1}) is particularly significant due to its high conformational dependence and sensitivity. In contrast, the adjacent Amide II and III regions are less dependent on secondary structure content. The Amide I region primarily arises from C=O stretching vibrations and out-of-phase CN stretching vibrations of the polypeptide backbone (Zhao et al., 2021). Each type of secondary structure contributes to absorption within a specific wavenumber range within the 1600–1700 cm^{-1} region. Despite being commonly used due to its strong signal, the Amide I region (1700 -1600 cm^{-1}) has limitations, such as strong interference from water vibrational bands, relatively unstructured spectral contours, and overlap of bands corresponding to various secondary structures. This peak includes components such as β-sheets, random structures, α-helix, and β-turns (Tiernan et al., 2020).

Due to differences in protein content and presence of other constituents such as fibre and starch, spectral intensity variations were notably pronounced in the Amide I, II, and III regions. The average absorption magnitude of pea and soy proteins was lower compared to whey and US-FBP. The Amide III region is generally considered less sensitive in protein IR spectra, with its bands primarily arising from NH bending and CN stretching vibrations, which are conformationally dependent (Barth, 2007). Although the basic structural characteristics of the proteins remained constant for all the proteins, partial changes occurred in the band intensities. This differences in band intensity may be attributed to the composition and processing history of the final ingredient as commercial proteins (soy and pea) are usually produced using extensive conditions compared to laboratory extracted proteins (Ma et al., 2022b; Nicolai & Chassenieux, 2019). As seen in Fig. 8C, the Amide A and B spectra effectively differentiate between the various protein samples. A

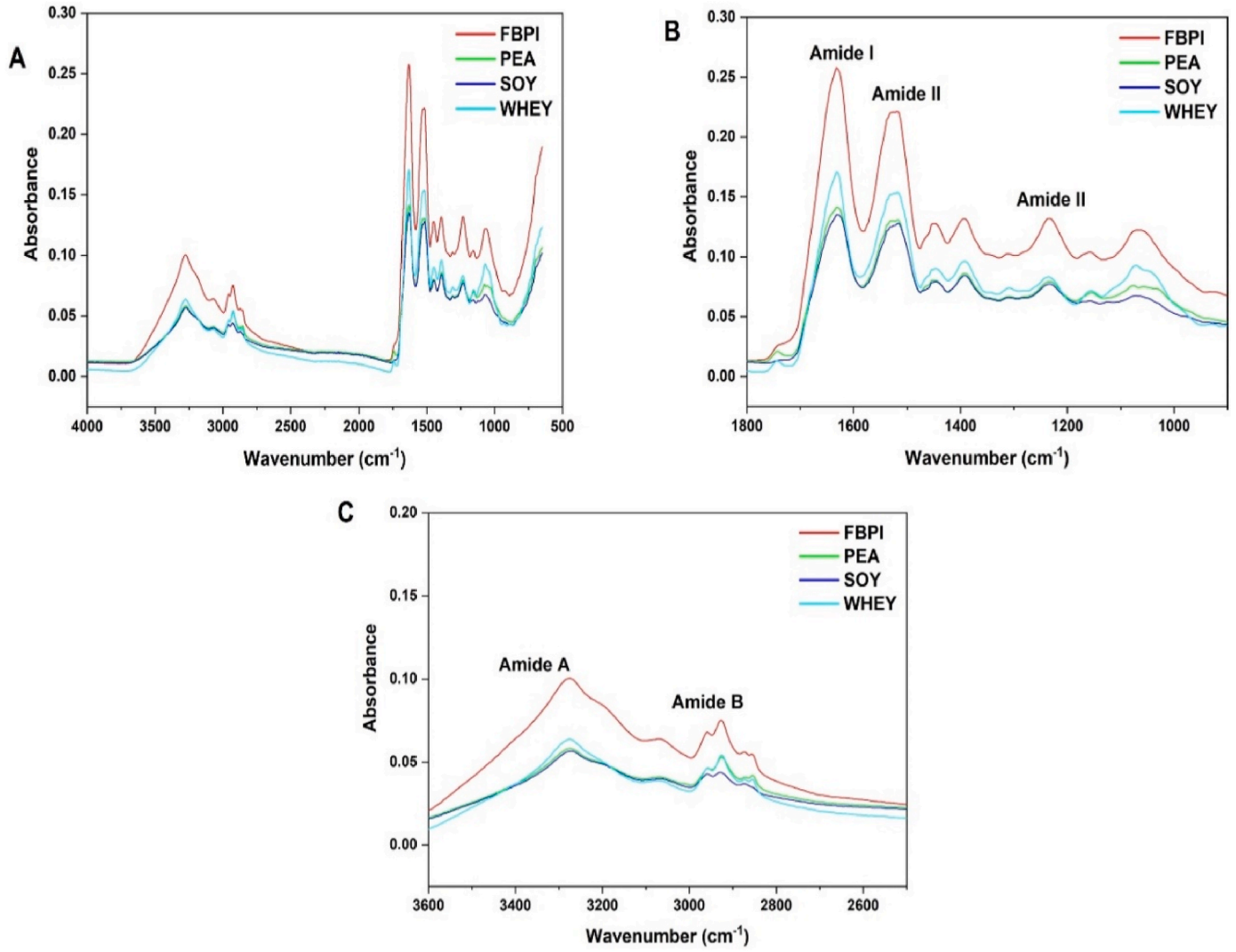

Fig. 8. FTIR spectra of protein isolate powders of faba bean, pea, soy and whey protein; (a) original spectra; (b) Amide I - III region 1800–900 cm $^{-1}$ and (c) Amide A and B region 1200–700 cm $^{-1}$. Average of replicates (n = 4).

major peak was observed around ~3300 and ~2900 cm^{-1}; however, this peak was less pronounced in soy, pea, and whey proteins compared to U-faba bean protein, likely due to their comparatively lower protein content.

4. Conclusion

This study offers a comprehensive multi-scale experimental review of the primary viscoelastic and structural properties of promising plant proteins for potential use in the development of next-generation foods. The rheological, functional, structural, and thermal behaviours of commercial proteins (soy and pea) were compared to those of ultrasound-extracted faba bean protein (US-FBP). Based on viscosity measurements, the proteins ranked in order of viscosity as soy (n = 0.32) > pea (0.56) > US-FBP (0.69), modelled by the power law and characterized by the consistency index (k) and power law index (n). Distinct gelling behaviours were observed among the plant proteins due to differences in molecular composition. The minimum gelation concentration was identified as 10 %, but gel strength varied, ranking U-faba bean > soy > pea. In situ gelation at 12 % showed a high G′ for US-FBP (G' = 2218 Pa) compared to soy (1458 Pa) and Pea (236.27 Pa). Structural studies using FTIR analysis showed distinct spectra intensity difference in the protein regions was observed in the order of US-FBP < soy < pea protein. Among the proteins, US-faba bean protein exhibited the lowest water-holding capacity at various concentrations compared to the commercial proteins. In conclusion, this work provides valuable insights into tailoring plant proteins and tuning textural properties for developing sustainable food products.

CRediT authorship contribution statement

Abraham Badjona: Writing – review & editing, Writing – original draft, Resources, Methodology, Investigation, Formal analysis, Data curation, Conceptualization. **Beatrice Cherono:** Writing – original draft, Methodology, Investigation. **Robert Bradshaw:** Writing – review & editing, Writing – original draft, Supervision, Resources, Project administration, Methodology, Funding acquisition, Formal analysis, Conceptualization. **Bipro Dubey:** Writing – review & editing, Writing – original draft, Supervision, Resources, Project administration, Methodology, Funding acquisition, Conceptualization.

Data availability statement

The data generated during the current study are available upon reasonable request.

Rights retention statement

Declaration of competing interest

The authors declare that they have no known competing financial interests or personal relationships that could have appeared to influence the work reported in this paper.

Acknowledgments

The authors would like to thank Jonny Shepherd, and the NCEFE team at Sheffield Hallam University for the guidance received when performing the experiments.

Data availability

Data will be made available on request.

References

Alting, A. C., Hamer, R. J., De Kruif, Paques, M., & Visschers, R. W. (2003). Number of thiol groups rather than the size of the aggregates determines the hardness of cold set whey protein gels. *Food Hydrocolloids, 17*(4), 469–479. https://doi.org/10.1016/S0268-005X(03)00023-7.

Ansari, S., Rashid, M. A. I., Waghmare, P. R., & Nobes, D. S. (2020). Measurement of the flow behavior index of Newtonian and shear-thinning fluids via analysis of the flow velocity characteristics in a mini-channel. *SN Applied Sciences, 2*(11). https://doi.org/10.1007/s42452-020-03561-w

Badjona, A., Bradshaw, R., Millman, C., Howarth, M., & Dubey, B. (2023). Faba beans protein as an Unconventional protein source for the food industry: Processing influence on nutritional, techno-functionality, and bioactivity. In *Food reviews international*. Taylor and Francis Ltd. https://doi.org/10.1080/87559129.2023.2245036.

Badjona, A., Bradshaw, R., Millman, C., Howarth, M., & Dubey, B. (2024a). Optimization of ultrasound-assisted extraction of faba bean protein isolate: Structural, functional, and thermal properties. Part 2/2. *Ultrasonics Sonochemistry, 110*, Article 107030. https://doi.org/10.1016/j.ultsonch.2024.107030

Badjona, A., Bradshaw, R., Millman, C., Howarth, M., & Dubey, B. (2024b). Response surface methodology guided approach for optimization of protein isolate from Faba bean. Part 1/2. *Ultrasonics Sonochemistry, 109*, Article 107012. https://doi.org/10.1016/j.ultsonch.2024.107012

Badjona, A., Bradshaw, R., Millman, C., Howarth, M., & Dubey, B. (2024c). Structural, thermal, and physicochemical properties of ultrasound-assisted extraction of faba bean protein isolate (FPI). *Journal of Food Engineering, 377*. https://doi.org/10.1016/j.jfoodeng.2024.112082

Barth, A. (2007). Infrared spectroscopy of proteins. *Biochimica et Biophysica Acta - Bioenergetics, 1767*(9), 1073–1101. https://doi.org/10.1016/j.bbabio.2007.06.004

Benoit, S. M., Afizah, M. N., Ruttarattanamongkol, K., & Rizvi, S. S. H. (2013). Effect of pH and temperature on the viscosity of texturized and commercial whey protein dispersions. *International Journal of Food Properties, 16*(2), 322–330. https://doi.org/10.1080/10942912.2011.552015

Bora, P. S., Brekke, C. J., & Powers, J. R. (1994). *Heat induced gelation of pea (pisum sativum) mixed globulins, vicilin and legumin*.

Bühler, J. M., Schlangen, M., Möller, A. C., Bruins, M. E., & van der Goot, A. J. (2022). Starch in plant-based meat replacers: A new approach to using endogenous starch from cereals and legumes. *Starch/Staerke, 74*, 1–2. https://doi.org/10.1002/star.202100157. John Wiley and Sons Inc.

Clark, A. H., Kavanagh, G. M., & Ross-Murphy, S. B. (2001). Globular protein gelationÐtheory and experiment. www.elsevier.com/locate/foodhyd.

Coimbra, L., Costa, I. M., Evangelista, J. G., & Figueiredo, A. (2023). Food allergens in oral care products. *Scientific Reports, 13*(1). https://doi.org/10.1038/s41598-023-33125-y

Farshi, P., Mirmohammadali, S. N., Rajpurohit, B., Smith, J. S., & Li, Y. (2024). Pea protein and starch: Functional properties and applications in edible films. *Journal of Agriculture and Food Research, 15*. https://doi.org/10.1016/j.jafr.2023.100927

Ferry, J. D. (1980). *Viscoelastic properties of polymers*. Wiley.

Hall, A. E., & Moraru, C. I. (2021). Structure and function of pea, lentil and faba bean proteins treated by high pressure processing and heat treatment. *LWT, 152*. https://doi.org/10.1016/j.lwt.2021.112349

Hayek, M. N., Harwatt, H., Ripple, W. J., & Mueller, N. D. (2021). The carbon opportunity cost of animal-sourced food production on land. *Nature Sustainability, 4*(1), 21–24. https://doi.org/10.1038/s41893-020-00603-4

Hua, Y., Cui, S. W., Wang, Q., Mine, Y., & Poysa, V. (2005). Heat induced gelling properties of soy protein isolates prepared from different defatted soybean flours. *Food Research International, 38*(4), 377–385. https://doi.org/10.1016/j.foodres.2004.10.006.

Jiménez-Munoz, L., Torp Nielsen, M., Roman, L., & Corredig, M. (2023). Variation of in vitro digestibility of pea protein powder dispersions from commercially available sources. *Food Chemistry, 401*. https://doi.org/10.1016/j.foodchem.2022.134178

Johansson, M., Karkehabadi, S., Johansson, D. P., & Langton, M. (2023). Gelation behaviour and gel properties of the 7S and 11S globulin protein fractions from faba bean (Vicia faba var. minor) at different NaCl concentrations. *Food Hydrocolloids, 142*. https://doi.org/10.1016/j.foodhyd.2023.108789

Kamani, M. H., Liu, J., Fitzsimons, S. M., Fenelon, M. A., & Murphy, E. G. (2024). Determining the influence of fava bean pre-processing on extractability and functional quality of protein isolates. *Food Chemistry X, 21*. https://doi.org/10.1016/j.fochx.2024.101200

Kaur, L., Mao, B., Beniwal, A. S., Abhilasha, Kaur, R., Chian, F. M., et al. (2022). Alternative proteins vs animal proteins: The influence of structure and processing on their gastro-small intestinal digestion. *Trends in Food Science and Technology, 122*, 275–286. https://doi.org/10.1016/j.tifs.2022.02.021. Elsevier Ltd.

Kyriakopoulou, K., Dekkers, B., & van der Goot, A. J. (2019). Plant-based meat analogues. In *Sustainable meat production and processing* (pp. 103–126). Elsevier. https://doi.org/10.1016/B978-0-12-814874-7.00006-7.

Lescinsky, H., Afshin, A., Ashbaugh, C., Bisignano, C., Brauer, M., Ferrara, G., et al. (2022). Health effects associated with consumption of unprocessed red meat: A burden of proof study. *Nature Medicine, 28*(10), 2075–2082. https://doi.org/10.1038/s41591-022-01968-z

Liang, Y., Wong, S. S., Pham, S. Q., & Tan, J. J. (2016). Effects of globular protein type and concentration on the physical properties and flow behaviors of oil-in-water emulsions stabilized by micellar casein-globular protein mixtures. *Food Hydrocolloids, 54*, 89–98. https://doi.org/10.1016/j.foodhyd.2015.09.024

Lyu, Z., Sala, G., & Scholten, E. (2022). Water distribution in maize starch-pea protein gels as determined by a novel confocal laser scanning microscopy image analysis method and its effect on structural and mechanical properties of composite gels. *Food Hydrocolloids, 133*. https://doi.org/10.1016/j.foodhyd.2022.107942

Ma, K. K., Greis, M., Lu, J., Nolden, A. A., McClements, D. J., & Kinchla, A. J. (2022a). Functional performance of plant proteins. *Foods, 11*(Issue 4). https://doi.org/10.3390/foods11040594. MDPI.

Ma, K. K., Greis, M., Lu, J., Nolden, A. A., McClements, D. J., & Kinchla, A. J. (2022b). Functional performance of plant proteins. *Foods, 11*(Issue 4). https://doi.org/10.3390/foods11040594. MDPI.

Ma, K. K., Grossmann, L., Nolden, A. A., McClements, D. J., & Kinchla, A. J. (2022). Functional and physical properties of commercial pulse proteins compared to soy derived protein. *Future Foods, 6*. https://doi.org/10.1016/j.fufo.2022.100155

Magrini, M. B., Anton, M., Chardigny, J. M., Duc, G., Duru, M., Jeuffroy, M. H., et al. (2018). Pulses for sustainability: Breaking agriculture and food sectors out of lock-in. *Frontiers in Sustainable Food Systems, 2*. https://doi.org/10.3389/fsufs.2018.00064

Mazumder, M. A. R., Panpipat, W., Chaijan, M., Shetty, K., & Rawdkuen, S. (2023). Role of plant protein on the quality and structure of meat analogs: A new perspective for vegetarian foods. *Future Foods, 8*. https://doi.org/10.1016/j.fufo.2023.100280. Elsevier B.V.

McClements, D. J. (2023). Modeling the rheological properties of plant-based foods: Soft matter physics principles. *Sustainable Food Proteins, 1*(3), 101–132. https://doi.org/10.1002/sfp2.1015

McClements, D. J., & Grossmann, L. (2021). The science of plant-based foods: Constructing next-generation meat, fish, milk, and egg analogs. *Comprehensive Reviews in Food Science and Food Safety, 20*(4), 4049–4100. https://doi.org/10.1111/1541-4337.12771. Blackwell Publishing Inc.

McClements, D. J., Newman, E., & McClements, I. F. (2019). Plant-based milks: A review of the science underpinning their design, fabrication, and performance. *Comprehensive Reviews in Food Science and Food Safety, 18*(6), 2047–2067. https://doi.org/10.1111/1541-4337.12505. Blackwell Publishing Inc.

Michel, F., Hartmann, C., & Siegrist, M. (2021). Consumers' associations, perceptions and acceptance of meat and plant-based meat alternatives. *Food Quality and Preference, 87*. https://doi.org/10.1016/j.foodqual.2020.104063

Nagy, R., Máthé, E., Csapó, J., & Sipos, P. (2021). Modifying effects of physical processes on starch and dietary fiber content of foodstuffs. *Processes, 9*(1), 1–16. https://doi.org/10.3390/pr9010017. MDPI AG.

Nicolai, T., & Chassenieux, C. (2019). Heat-induced gelation of plant globulins. *Current Opinion in Food Science, 27*, 18–22. https://doi.org/10.1016/j.cofs.2019.04.005. Elsevier Ltd.

Okeudo-Cogan, M. C., Murray, B. S., Ettelaie, R., Connell, S. D., Radford, S. J., Micklethwaite, S., et al. (2023). Understanding the microstructure of a functional meat analogue: Demystifying interactions between fungal hyphae and egg white protein. *Food Hydrocolloids, 140*. https://doi.org/10.1016/j.foodhyd.2023.108606

Osen, R., Toelstede, S., Wild, F., Eisner, P., & Schweiggert-Weisz, U. (2014). High moisture extrusion cooking of pea protein isolates: Raw material characteristics, extruder responses, and texture properties. *Journal of Food Engineering, 127*, 67–74. https://doi.org/10.1016/j.jfoodeng.2013.11.023

Paximada, P., Howarth, M., & Dubey, B. N. (2021). Double emulsions fortified with plant and milk proteins as fat replacers in cheese. *Journal of Food Engineering, 288*. https://doi.org/10.1016/j.jfoodeng.2020.110229

Ren, W., Xia, W., Gunes, D. Z., & Ahrné, L. (2024). Heat-induced gels from pea protein soluble colloidal aggregates: Effect of calcium addition or pH adjustment on gelation behavior and rheological properties. *Food Hydrocolloids, 147*. https://doi.org/10.1016/j.foodhyd.2023.109417

Schlangen, M., Taghian Dinani, S., Schutyser, M. A. I., & van der Goot, A. J. (2022a). Dry fractionation to produce functional fractions from mung bean, yellow pea and

cowpea flour. *Innovative Food Science and Emerging Technologies, 78*. https://doi.org/10.1016/j.ifset.2022.103018

Schlangen, M., Taghian Dinani, S., Schutyser, M. A. I., & van der Goot, A. J. (2022b). Dry fractionation to produce functional fractions from mung bean, yellow pea and cowpea flour. *Innovative Food Science and Emerging Technologies, 78*. https://doi.org/10.1016/j.ifset.2022.103018

Schmid, E. M., Farahnaky, A., Adhikari, B., Savadkoohi, S., & Torley, P. J. (2024). Investigation into the physiochemical properties of soy protein isolate and concentrate powders from different manufacturers. *International Journal of Food Science and Technology, 59*(3), 1679–1693. https://doi.org/10.1111/ijfs.16923

Shand, P. J., Ya, H., Pietrasik, Z., & Wanasundara, P. K. J. P. D. (2007). Physicochemical and textural properties of heat-induced pea protein isolate gels. *Food Chemistry, 102*(4), 1119–1130. https://doi.org/10.1016/j.foodchem.2006.06.060.

Shrestha, S., Hag, L. van 't, Haritos, V., & Dhital, S. (2023). Rheological and textural properties of heat-induced gels from pulse protein isolates: Lentil, mungbean and yellow pea. *Food Hydrocolloids, 143*. https://doi.org/10.1016/j.foodhyd.2023.108904

Sim, S. Y. J., Srv, A., Chiang, J. H., & Henry, C. J. (2021). Plant proteins for future foods: A roadmap. *Foods, 10*(Issue 8). https://doi.org/10.3390/foods10081967. MDPI AG.

Snel, S. J. E., Bellwald, Y., van der Goot, A. J., & Beyrer, M. (2022). Novel rotating die coupled to a twin-screw extruder as a new route to produce meat analogues with soy, pea and gluten. *Innovative Food Science and Emerging Technologies, 81*. https://doi.org/10.1016/j.ifset.2022.103152

Stevenson, P. (2023). Links between industrial livestock production, disease including zoonoses and antimicrobial resistance. *Animal Research and One Health, 1*(1), 137–144. https://doi.org/10.1002/aro2.19

Sun, X. D., & Arntfield, S. D. (2012). Molecular forces involved in heat-induced pea protein gelation: Effects of various reagents on the rheological properties of salt-extracted pea protein gels. *Food Hydrocolloids, 28*(2), 325–332. https://doi.org/10.1016/j.foodhyd.2011.12.014

Tanger, C., Andlinger, D. J., Brümmer-Rolf, A., Engel, J., & Kulozik, U. (2021). Quantification of protein-protein interactions in highly denatured whey and potato protein gels. *MethodsX, 8*. https://doi.org/10.1016/j.mex.2021.101243

Tiernan, H., Byrne, B., & Kazarian, S. G. (2020). ATR-FTIR spectroscopy and spectroscopic imaging for the analysis of biopharmaceuticals. *Spectrochimica Acta - Part A: Molecular and Biomolecular Spectroscopy, 241*. https://doi.org/10.1016/j.saa.2020.118636. Elsevier B.V.

van der Sman, R. G. M., & van der Goot, A. J. (2023). Hypotheses concerning structuring of extruded meat analogs. *Current Research in Food Science, 6*. https://doi.org/10.1016/j.crfs.2023.100510. Elsevier B.V.

Weathers, S. T., Caviola, L., Scherer, L., Pfister, S., Fischer, B., Bump, J. B., et al. (2020). Quantifying the valuation of animal welfare among Americans. *Journal of Agricultural and Environmental Ethics, 33*(2), 261–282. https://doi.org/10.1007/s10806-020-09824-1

Wittek, P., Zeiler, N., Karbstein, H. P., & Emin, M. A. (2020). Analysis of the complex rheological properties of highly concentrated proteins with a closed cavity rheometer. *Applied Rheology, 30*(1), 64–76. https://doi.org/10.1515/arh-2020-0107

Xia, W., Siu, W. K., & Sagis, L. M. C. (2021). Linear and non-linear rheology of heat-set soy protein gels: Effects of selective proteolysis of β-conglycinin and glycinin. *Food Hydrocolloids, 120*. https://doi.org/10.1016/j.foodhyd.2021.106962

Xia, W., Zhu, L., Delahaije, R. J. B. M., Cheng, Z., Zhou, X., & Sagis, L. M. C. (2022). Acid-induced gels from soy and whey protein thermally-induced mixed aggregates: Rheology and microstructure. *Food Hydrocolloids, 125*. https://doi.org/10.1016/j.foodhyd.2021.107376

Yang, J., Lorenzetti, R. L., Bing, D., Zhang, S., Lu, J., & Chen, L. (2023). Composition, functionalities, and digestibility of proteins from high protein and normal pea (Pisum sativum) genotypes. *Sustainable Food Proteins, 1*(1), 4–15. https://doi.org/10.1002/sfp2.1005

Zhao, J., Cui, J. K., Chen, R. X., Tang, Z. Z., Tan, Z. L., Jiang, L. Y., et al. (2021). Real-time in-situ quantification of protein secondary structures in aqueous solution based on ATR-FTIR subtraction spectrum. *Biochemical Engineering Journal, 176*. https://doi.org/10.1016/j.bej.2021.108225